Petroleum Research 7 (2022) 372–383

Contents lists available at ScienceDirect

Petroleum Research

journal homepage: http://www.keaipublishing.com/en/journals/petroleum-research/

Evaluation of influential parameters for supersonic dehydration of natural gas: Machine learning approach

Emmanuel E. Okoro [a, b, *], Uyiosa Igbinedion [b], Victor Aimikhe [a], Samuel E. Sanni [c], Okorie E. Agwu [d]

[a] Department of Petroleum and Gas Engineering, University of Port Harcourt, Nigeria
[b] Department of Petroleum Engineering, Covenant University, Ota, Nigeria
[c] Department of Chemical Engineering, Covenant University, Ota, Nigeria
[d] Department of Petroleum Engineering, University of Uyo, Nigeria

ARTICLE INFO

Article history:
Received 21 September 2021
Received in revised form
8 December 2021
Accepted 9 December 2021
Available online 14 December 2021

Keywords:
Supersonic separator
Machine learning model
Natural gas dehydration
Separation efficiency

ABSTRACT

The supersonic dehydration of natural gas is gaining more attention due to its numerous advantages over the conventional natural gas dehydration technologies. However, supersonic separators have seen minimal field applications despite the multiple benefits over other gas dehydration techniques. This has been mostly attributed to the uncertainty in ascertaining the design and operating parameters that should be monitored to ensure optimum dehydration of the supersonic separation device. In this study, the decision tree machine learning model is employed in investigating the effects of design and operating parameters (inlet and outlet pressures, nozzle length, throat diameter, and pressure loss ratio) on the supersonic separator performance during dehydration of natural gas. The model results show that the significant parameters influencing the shock wave location are the pressure loss ratio and nozzle length. The former was found to have the most significant effect on the dew point depression. The dehydration efficiency is mainly dependent on the pressure loss ratio, nozzle throat diameter, and the nozzle length. Comparing the machine learning model-accuracy with a 1-D iterative model, the machine learning model outperformed the 1-D iterative model with a lower mean average percentage error (MAPE) of 5.98 relative to 15.44 as obtained for the 1-D model.

1. Introduction

Over decades, the production of natural gas has been on a steady increase, and the growth in output is expected to increase even more as cleaner and more environmentally friendly sources of energy are sought (Karimi and Abdi, 2009). According to the US Department of Energy, gas demand is expected to increase by about 31% between 2015 and 2035 (Alnoush and Castier, 2019). Natural gas comprises of methane, ethane, propane (Wajdi and Marcelo, 2019), n-butane, isobutene, carbon dioxide, nitrogen, isopentane, oxygen, n-pentane, hydrogen, helium, hexane, hydrogen sulphide and mercaptans (Sanni et al., 2020). The associated liquids are usually separated from the gas stream by using phase separators, which operate on the density difference principle. At the same time, the entrained liquid must be removed via other process systems. Traditional natural gas dehydration methods usually entail high capital and operating costs (Ding et al., 2020). Relevant units may contain rotating components, which usually require complex crew operations, safety issues, and frequent schedules for maintenance (Othman et al., 2020). The addition of chemicals, such as hydrate inhibitors in traditional methods, poses serious environmental problems (Wajdi and Marcelo, 2018). Conventional natural gas dehydration uses a contactor-regenerator column set up with a hygroscopic liquid desiccant (Wajdi and Marcelo, 2019).

Due to liquid entrainment in the gas phase which renders the gas wet, there is need to separate these phases. Any free fluid present is usually separated using phase separators, but the entrained liquid phase will require an additional removal process (Yang et al., 2014b). Some conventional methods currently being used to separate natural gas include absorption, adsorption, refrigeration, and cryogenic separation (Yang et al., 2014b).

* Corresponding author. Department of Petroleum and Gas Engineering, University of Port Harcourt, Nigeria.
E-mail address: emeka.okoro@uniport.edu.ng (E.E. Okoro).

https://doi.org/10.1016/j.ptlrs.2021.12.005

Absorption involves the use of absorbents, and these absorbents include ethylene glycol, $CaCl_2$, $(HOCH_2CH_2)_2O$, triethylene glycol, and $C_8H_{18}O_5$ (Cao and Bian, 2019). The ease of absorbent regeneration and flexible treatment ability are some of the advantages of the absorption method, but the vast equipment required makes absorption process noncommercially viable (Xuewen and Jiang, 2019).

Adsorption, on the other hand, is a surface phenomenon that uses a solid or liquid absorber to absorb the absorbate. Common solid adsorbents in the industry include activated alumina, molecular sieves and silica gel (Zhang et al., 2014). Shallow dew points can be achieved using these conventional solid adsorbents as they are also suitable for cryogenic separation processes, which require very low gas content feed. Still, substantial investment and high gas pressure loss are some of the disadvantages (Xuewen and Jiang, 2019). Membrane separation technology also can be used for adsorption where the gas mixture is effectively separated by a synthetic membranes made mostly from polymers or other hybrid materials (Ruiz, 2015). This technology holds significant potentials because of some advantages including process simplicity, reduced land use and secondary pollution. However, large-scale industrial applications for membrane separation still has significant problems, including significant hydrocarbons loss during the process (Xuewen and Jiang, 2019).

Supersonic separator technology does not include rotating (dynamic) components, and it does not require the addition of chemicals (Marcelo, 2016). The primary components of a supersonic separator include a swirling device as well as the de Laval converging-diverging nozzle alongside a diffuser extension. Niknam et al. (2019) investigated the effect of supersonic nozzle geometry on separation efficiency with specific interest on the internal body of the nozzles. They observed that a small inner body radius has no significant effect on the position of the shockwave. Also, an enhanced physical phase separation was observed for higher stability swirling velocity magnitude. The swirling device converts axial velocity to angular velocity, and this helps to enhance centrifugal separation of the condensed stream phase (Wajdi and Marcelo, 2019). Niknam et al. (2018a) also investigated nozzle performance and cooling capacity in terms of temperature, pressure and gas type in a fixed geometry. And they highlighted that the criterion for nozzle performance is provided by prediction of exact shock wave position. They further noted that the shock wave position is unchanged during alteration of fluid type or pressure scale. The nozzle is where condensation occurs at supersonic speed. During this process, water and other possible condensates are separated from the stream (Niknam et al., 2016). The performance of a supersonic separator has been studied using numerical simulation and computational fluid dynamics techniques while considering the effects of inlet pressure and inlet temperature. Supersonic separators have seen minimal field applications despite the numerous advantages they provide over other gas dehydration techniques. One of the major problems yet to be resolved is the effective monitoring of the design and operating parameters for optimum dehydration throughout the nozzle's design life (Mahmoodzadeh and Shahsavand, 2013). Most of the published studies on supersonic separation of Natural gas mainly investigated the factors responsible for the effective separation of the gas without establishing the level of significance those factors had on the dehydration efficiency, dew point suppression, and shockwave location. These levels of significance are essential for the efficient design and operation of the supersonic dehydration system. Also, the published studies only considered a limited number of factors and a small range of their operating conditions. Given the full range of possible conditions, the use of machine learning techniques makes it possible to simulate this range of conditions.

This study investigates the performance of a supersonic separator during natural gas dehydration using the decision tree machine learning model while also exploring the effect of inlet and outlet pressure, nozzle length, throat diameter, and pressure loss ratio on the water removal process. Supersonic separator technique benefits (such as absence of moving parts, low power consumption, pressurized product, etc) have influenced interest in Natural gas application over the past decade. The challenge has been on how to identify and optimize the inlet conditions and parameters for sustainability and profitability. For optimal performance of supersonic separator, the is need to identify feed conditions to maintain supersonic flow throughout the nozzle diverging section. The decision tree creates a reliable and straightforward model that overcomes the shortcomings of numerical and 1-D models, such as the neglect of the swirling effect and the inability to consider two-phase flow. Unlike previous numerical models, the proposed artificial method covers a number of boundary conditions and nozzle geometry since sonic conditions at supersonic separator throat is mandatory for operation. Literature has shown that identifying some of the optimum inlet conditions have posed some technical issues in the field practice for this technology (Cao and Bian, 2019). This study is aimed at predicting the effect of the dynamic parameters of the nozzle inlet and outlet on the selective dehydration of natural gas with respect to the separation efficiency.

2. Supersonic gas separation

The basic principle of the supersonic separation is the throttling process, commonly known as the Joule-Thomson (JT) process i.e. the J-T effect. Joule Thomson Valve is a throttle valve or constant flow design device used to cause large pressure drops and large temperature drops. The compressed gas extends from high to low pressure with constant enthalpy, thus converting the potential energy into kinetic energy; thereby accelerating the gas to supersonic speed limit (Othman et al., 2020). The changes in gas temperature during expansion depend not only on the initial and final pressures, but also on how expansion occurs. The two factors that can change the fluid temperature during adiabatic expansion are: change in internal energy or conversion between kinetic and potential internal energy (Wang, 2020).

Static vanes are installed at the nozzle inlet so as to create a swirling gas flow. The resulting water droplet is separated by centrifugal force applied to the nozzle wall. The thin film of water on the walls moves in the direction of flow towards the separation channel. The separation duct leads to the heated degassing separator. From there, the return of slip gas to the mainstream, and condensed water is removed (Karimi and Abdi, 2009). After separating the water, it is very important to restore the gas pressure by altering the kinetic energy; thus, the imposition of a shock wave. Shock waves usually occur when the speed of the gas exceeds the speed of generated sound. With supersonic nozzles, shock waves are generated by a rapid increase in the diameter of the nozzle downstream the nozzle throat (diffuser). Fig. 1 shows the volume, pressure, and temperature profile of the gas flowing through a supersonic nozzle. Due to the sudden drop in temperature and pressure, the water vapour in the gas stream condenses and falls as droplets, while the methane gas continues to flow through the nozzle-channel (Okimoto and Brouwer, 2002).

In fact, the Joule-Thomson effect is achieved by expanding the gas through a valve that is well insulated to prevent heat transfer to or from the gas. In the supersonic gas separation technique, the flow passes through a nozzle at its throat, where it is accelerated to a high supersonic speed (Cao and Bian, 2019). Due to the rapid expansion at the nozzle outlet, the desired condensate is formed as a mist. The swirling centrifugal energy transport these film-like

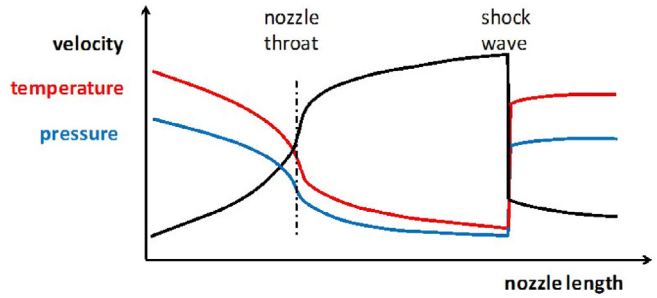

Fig. 1. PVT profile of a gas passing through the Supersonic Nozzle (Netusil and Ditl, 2012).

liquids towards the wall, where they flow through a proper structure and are evacuated with some of the sliding gas. The now dry gas flows continuously through the anti-swirl device and the diffusers (Niknam et al., 2018b). Here the flow is reduced, and the kinetic energy is converted to pressure, thus, about 75–80% of the inlet pressure is restored. To achieve supersonic gas velocity, the inlet diameter must be at least $\sqrt{5}$ times the nozzle throat-diameter, and the converging length must be greater than or equal to the throat diameter (Wen et al., 2011). Increasing the nozzle length increases separation efficiency due to an increase in the nozzle wall surface area required for particle collision. On the other hand, a longer nozzle length than the critical length, will increase temperature due to friction loss, which in turn causes the evaporation of already condensed (separated) liquids, leading to decreased separation efficiency (Alnoush and Castier, 2019). Consequently, there should be an optimal or critical length of 10 times the throat diameter for optimum performance.

Separation is enhanced by centrifugal forces, which separate the droplets on the walls of the nozzle. Dry gas continues to move forward while the liquid phase (usually with some slip gas) is separated. Repeated swirls create centrifugal forces, and the higher the centrifugal force, the easier it is for droplets to drop to the wall to achieve separation (Bian et al., 2019). High-velocity inform higher swirling force that help separate liquid droplets onto the wall of the nozzle. Reducing swirling intensity leads to a reduction in centrifugal force which subsequently results in lower separation efficiencies. Swirls can be moderated by regulating the vanes at the nozzle inlet to achieve optimum low temperatures and moderate centrifugal forces for the separation process (Yang and Wen, 2017).

An optimal swirling force is required for the best separation; not too strong to avoid energy losses and not too weak to cause a reduction in centrifugal forces. Shock waves are produced to recover the initial pressure of the gas. This is achieved when supersonic velocities (i.e. Mach numbers >1 but less than 5) change to sonic velocities (i.e. Mach number = 1) caused by rapid enlargement of the nozzle diameter (Castier, 2014); for hyper sonic flows, the Mach number >5, while for subsonic flow, the Mach number is < 1), at static condition Mach number = 0. The existence of shockwaves increases the swirl intensity of droplets needed for efficient separation. The gas expansion results in a sufficient temperature drop that reaches the water vapour's dew point temperature in the gas. However, a higher inlet pressure delivers more energy necessary for maintaining the supersonic speed required for efficient separation. Furthermore, the temperature and pressure drop required for an efficient separation in the supersonic nozzle, increases with the pressure loss ratio.

The term supersonic is used to describe velocities that exceed the speed of sound (that is, Mach >1 but less than 5). The Mach number from literature is the moving object's velocity through a medium divided by the sound velocity in air. Mach number is often used for both moving objects and fast flowing liquids within channels. It is a number that cannot be measured because it is defined as the ratio of two velocities, thus, it is a dimensionless number. Since the sound velocity increases with temperature, the actual moving object's velocity at Mach 1 depends on the surrounding liquid's temperature. Mach number is very useful in characterizing the velocity of moving fluids because the fluid properties are similar when the Mach number is constant (Yang et al., 2014).

3. Methodology

Machine learning has had a significant impact on data-driven research methods today. Depending on the problem to be solved and the nature of the data available, different machine learning models can be used. To determine the optimum operating conditions and design for the supersonic separator, six variables (nozzle length, input pressure, output pressure, input temperature, nozzle diameter, and pressure loss ratio) considered to determine three target outputs (shock wave location, dew point depression and separation efficiency). These outputs are good indicators of the separator's performance (Xiao et al., 2009). This application was created as a supervised learning problem, and a data was created containing the desired results so that machine learning could solve the problem. A supervised machine learning task could be a classification problem or a regression problem. For regression problems, the goal is to predict a continuous or a real number. Classification and regression tasks can easily be distinguished by checking for continuity in the output. Whenever there is continuity amongst the possible outcomes, the problem is then a regression problem.

The task presented in this study is a regression problem since all outputs are continuous. Two different supervised learning algorithms for regression are used to build the models in this study. The decision tree is used for the modeling, and support vector machines are used for validation. Experimental data from existing literature was gathered and used to build a robust model that can be used for forecasting the performance of the supersonic separator under various operating conditions. The following equations define the output parameters (Ding et al., 2020);

Dew point depression

$$\Delta Td = Td_{in} - Td_{out} \tag{1}$$

where Td_{in} is the inlet gas dew point temperature, and Td_{out} .the separator-outlet dew point temperature.

Separation efficiency

$$\frac{Q_{dry}}{Q_{in}} \times 100\% = \frac{Q_{in} - Q_{wet}}{Q_{in}} \times 100\% \tag{2}$$

where Q_{in}, Q_{dry}, Q_{wet} are the inlet, dry and wet gas mass flow rates of the outlets, respectively.

Pressure loss ratio.

The pressure loss ratio input parameter is defined mathematically by equation (3);

$$\mathrm{Pr} = \frac{P_{in} - P_{out}}{P_{in}} \tag{3}$$

Where Pr, P_{in}, P_{out} represent Pressure loss ratio, inlet pressure, and outlet pressure.

3.1. Data description

Data obtained from Karimi and Abdi (2009), Yang et al. (2014), and Jing et al. (2014) were used in the DT-modeling, and Table 1 shows a sample of the data.

3.2. Data characteristics

The data set characteristics determine to a large extent which machine learning algorithm should be used, as some algorithms perform better than others for a given dataset. The following properties characterize the supersonic modeling dataset;

(1) Low dimensional
(2) All variables are continuous, not categorical
(3) Three target outputs
(4) Six input variables
(5) Variables have different scaling

The properties given above are why the decision tree and support vector machines are used for the modeling exercise. Given the wide range of possible operating conditions on the field, a wide range of input features were also considered, as shown in Table 2. A total of 112 data points were collected, and split into 70%, 15%, and 15% for training, testing and validation respectively.

Table 2 also shows the statistical details of the input parameters. It shows 0.1, 7, 1,0.15, 274.15 and 12.7 are the minimum of the observations for nozzle length, pressure-in and out, pressure loss ratio, temperature-in, and throat diameter; while 0.7, 700, 490, 0.86, 373, and 36.71 are the maximum of the observations for nozzle length, pressure-in and out, pressure loss ratio, temperature-in, and throat diameter respectively. The mode which is the value that occurs most often, the range that is simply the maximum observation minus the minimum value and median (number that is in the middle of the observations) are all tabulated in Table 2 for the input parameters used for the investigation. 95%, 99% and 99.9% confidence limits of the input variables were also determined. These are the numbers at the upper and lower end of a confidence interval. Setting 99.9% confidence limits means that if you took repeated random samples are taken repeatedly from the input variables and the mean calculated; the confidence limits for each input parameter values, the confidence interval for 99.9% of the variables would include the parametric mean.

3.3. Computing resources

Python is a popular and widely used tool for many data science and machine learning applications. Python has libraries for data loading, statistics analysis, natural language editing, image editing, visualization, and so on. Libraries such as scikit-learn, matplotlib, pandas, and NumPy were used in this study.

3.4. Modelling workflow

Machine learning and data analysis are fundamentally iterative processes. Machine learning workflows define which phases are implemented during a machine learning project. The typical phases include data collection, data pre-processing, building datasets, model training and refinement, evaluation, and deployment to production. Depending on the model to be used, the data might require pre-processing, wherein an appropriate technique is used to bring all features in the dataset to the same scale. All pre-processing techniques are available in the *sklearn pre-processing* class in the scikit-learn package. A suitable algorithm is then selected, and a model is built using the training dataset. The performance of the built model is then evaluated using the test dataset. The results given by the training and test data accuracy are used in determining how well the model has performed on the given dataset.

3.5. Decision tree

Decision trees are often used for regression problems. First of all, they learn a hierarchy of problems that lead to solutions. In the machine learning, these sets of logical questions are called tests (as opposed to test sets, which are the data used to test how general a proposed model is). As in this study, the data are presented mainly as a continuous function. To create the tree, the algorithm examines all possible tests to find the most informative one for the target variable. The data is then shared along that axis. Basically, the test is a division of the portion of the data being considered along one axis. The recursive data division is repeated until each module area (each decision tree sheet) contains only one target value (regression value). The leaves in a tree that contain data points with the same target value are called *pure*. The partitioning of a dataset might look like the chart shown in Fig. 2.

3.6. Controlling the complexity of decision trees (preventing model overfitting)

The goal of supervised learning is to create a model using training data and to accurately predict new unseen data with the same characteristics as the training set used. Training sets can be generalized to test sets if the proposed model can accurately predict hidden data. The goal is to build a model that can generalize as accurately as possible. There are two general strategies for preventing over-adjustment in literature; (1) avoid creating the tree early, and (2) create the tree and then collapse or delete the nodes that contains few information. If a decision tree's depth is not restricted, the tree can become arbitrarily deep and complex.

The process of generating the decision tree is the process of continuously optimizing the division parameters to minimize the loss function. In the process of decision tree generation, the parameters of the decision tree will gradually be optimized to the

Table 1
Sample of data used for this study.

Ref	Nozzle length (m)	P_{in} (bar)	P_{out} (bar)	P_r	T_{in} (K)	Throat Diameter (mm)	Shock location (x/D)	Dew point depression (°C)	Separation efficiency (%)
Karimi and Abdi (2009)	0.12	300	210	0.30	274.15	12.70	0.85	19.54	30.34
Karimi and Abdi (2009)	0.12	300	210	0.30	293.15	15.94	0.85	20.35	31.43
Yang et al. (2014)	0.12	300	210	0.30	313.15	16.30	0.91	18.25	29.35
Jing et al. (2014)	0.12	300	210	0.30	333.15	17.40	0.93	19.85	30.63
Jing et al. (2014)	0.12	300	249	0.17	293.15	21.00	0.68	7.20	7.75

Table 2
Descriptive statistical analysis of the flow parameters, nozzle length and throat diameter.

Parameters	Nozzle length (m)	P_{in} (bar)	P_{out} (bar)	P_r	T_{in} (K)	Throat Diameter (mm)
mean	0.283	198.452	140.925	0.350	300.515	19.773
std	0.252	160.158	113.391	0.177	18.809	7.966
Median	0.12	200	150	0.70	293.15	16.30
Mode	0.12	300	210	0.75	293.15	12.70
Range	0.60	693	489	0.71	98.85	24.01
min	0.1	7	1	0.15	274.15	12.7
25%	0.11	100	66	0.25	293.15	15.94
50%	0.12	200	150	0.3	293.15	16.3
75%	0.6	300	210	0.385	300	21
max	0.7	700	490	0.86	373	36.71
CI 95%	0.194–0.371	142–255	101–181	0.288–0.413	294–307	17–22.6
CI 99%	0.166–0.4	124–273	88.4–193	0.268–0.432	292–309	16.1–23.5
CI 99.9%	0.134–0.432	104–293	73.9–208	0.245–0.455	289–312	15.1–24.5

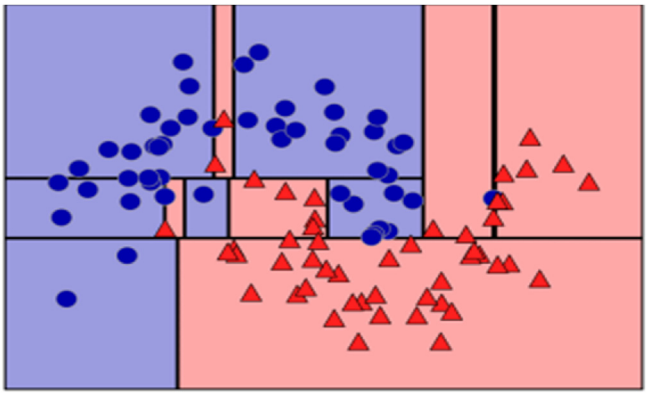

Fig. 2. Decision boundary of a tree after the partitioning of the dataset.

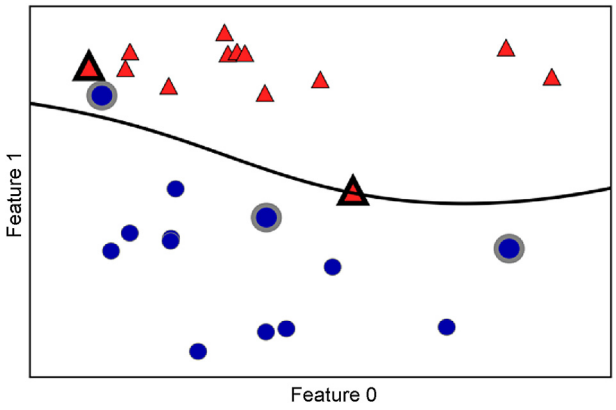

Fig. 3. Decision Boundary and Support Vectors found by an SVM.

parameters that have lowest loss function, the model can inevitably become complicated, but the complex model structure does not improve the prediction accuracy. To improve the prediction accuracy, it is necessary to take pruning operations on the model. The algorithm consists of two steps:

(1) Decision tree generation: Generate the corresponding decision tree based on the training data set, and the generated model structure should be as large as possible.
(2) Decision tree pruning: Prune the decision tree model based on the validation data set and select the best subtree structure.

In building the supersonic separator model, the following two parameters are set to ensure a model that will generalize well on the test data: (1) Random State, and (2) Maximum depth. One benefit of decision trees is that it does not require so much parameter tuning, and thus, practical models can be built quickly.

3.7. Support vector machines (SVM)

Another supervised learning algorithm used in this study is the support vector machine. The kernel support vector machines (or simply SVMs) is an addition to the linear support vector machines that allows the development of more complex models. During training, SVM learns the importance of each training data points that represents a decision limit between classes in the dataset. Fig. 3 shows the decision limits made by the SVM, it is marked in black, and the support vector is a larger dot with a wide border. The distance from each support vectors is measured to make a prediction from the new end. The decision is based on the distances from the support vector and the importance of the support vectors used for the training.

3.7.1. Preprocessing data for SVMs

SVMs often works well, but it is sensitive to parameters' configuration and data scaling. They require that all functions be placed on the same scale. The dataset used for this study have features changing on different scales. The maximum and minimum values of each component in the dataset are presented in Fig. 4. It

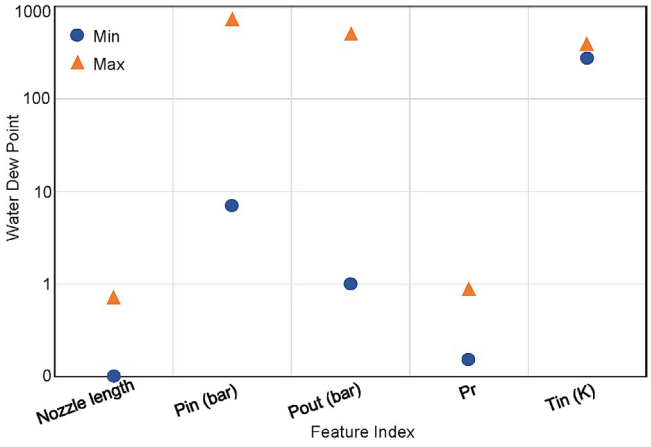

Fig. 4. Feature ranges for the supersonic modeling dataset.

shows that the dataset features are of entirely different orders of magnitude (the y-axis is on a logarithmic scale). It can pose serious problems for the kernel SVM. One way to solve this problem is to redefine each function on the same scale. The standard SVM kernel scale method was to scale the data so that all functions ranged from 0 to 1. This was done using the MinMaxScaler pre-processing method, and this was calculated manually using equation (4).

$$X_{train_{scaled}} = \frac{X_{train} - minimum}{range} \tag{4}$$

Table 3 shows the effect of scaling the data using the MinMax scaler. All values are between 0 and 1, hence putting all variables on the same scale. The SVM model built with the scaled data would produce better results.

3.7.2. HyperParameters applied in this study

The hyperparameters for the Support Vector Regreessor are: **C:** Parameter C is a regularization parameter. This limits the weight of each point, and a small C value means a very restricted model where each data point can have very limited effects. **Gamma:** It determines the degree of importance of adjacent points. **Epsilon:** It specifies the epsilon-tube within which no penalty is associated in the training loss function with points predicted within a distance epsilon from the actual value. **Tol:** Tolerance for stopping criterion. **Max_iter:** Hard limit on iterations within solver, or −1 for no limit. **Kernel:** Specifies the kernel type to be used in the algorithm. It must be one of 'linear', 'poly', 'rbf', 'sigmoid', 'precomputed' or a callable. If none is given, 'rbf' will be used. If a callable is given it is used to precompute the kernel matrix.

A random forest is a meta estimator that fits a number of classifying decision trees on various sub-samples of the dataset and uses averaging to improve the predictive accuracy and control over-fitting. These include: **Max_depth:** The maximum depth of the tree. If None, then nodes are expanded until all leaves are pure or until all leaves contain less than min_samples_split samples. **Criterion:** The function to measure the quality of a split. Supported criteria are "mse" for the mean squared error, which is equal to variance reduction as feature selection criterion, and "MAE" for the mean absolute error. **N_estimators:** The number of trees in the forest. **Max_features:** The number of features to consider when looking for the best split. **N_jobs:** The number of jobs to run in parallel. Fit, predict, decision path and apply are all parallelized over the trees. **Ccp_alpha:** Complexity parameter used for Minimal Cost-Complexity Pruning. The subtree with the largest cost complexity that is smaller than ccp_alpha will be chosen.

Gradient Boosting Regressor hyperparameters includes: **N_estimators:** The number of boosting stages to perform. Gradient boosting is fairly robust to over-fitting so a large number usually results in better performance. **Learning_rate:** Learning rate shrinks the contribution of each tree by learning_rate. There is a trade-off between learning_rate and n_estimators. **Max_depth:** Maximum depth of the individual regression estimators. The maximum depth limits the number of nodes in the tree. **Loss:** Loss function to be optimized. 'ls' refers to least squares regression. 'lad' (least absolute deviation) is a highly robust loss function solely based on order information of the input variables. 'huber' is a combination of the two. 'quantile' allows quantile regression. While that of the Extra Tree Regressor includes: **N_estimators:** This is the number of trees in the forest. **Cc_alpha:** Complexity parameter used for Minimal Cost-Complexity Pruning. The subtree with the largest cost complexity that is smaller than ccp_alpha will be chosen.

3.8. Correlation matrix

The relationship between all inputs and outputs is shown in the correlation matrix (Fig. 5). A correlation matrix shows correlation coefficients between variables considered in this study. The matrix was computed using the standard Pearson correlation coefficient, and the results were plotted as a heatmap. The correlation coefficient statistical significance is set between +1 and −1, which was colour-code according to the correlation statistics (light to dark) indicating a strong forward correlation or a weak/strong inverse correlation. Positive correlations are displayed in shades of green and negative correlation in shades of red/orange colour. Worthy to note is the relationship between the pressure loss ratio and the three target outputs. The pressure loss ratio has been determined to be the most important of all input variables, hence the focus on this parameter. There is a direct relationship between the pressure loss ratio and the three outputs (dew point depression, separation efficiency, and shockwave location).

3.9. Model validation

Statistical Error Analysis of the Applied Models:

Root Mean Squared Error, Mean Absolute Error, Mean Squared Error and Mean Absolute Percentage Error were the statistical error analysis tools used for this study, and they are mathematically presented as equations (5)–(8) respectively.

$$RMSE = \sqrt{\sum_{i=1}^{n} \frac{(\widehat{y}_i - y_i)^2}{n}} \tag{5}$$

$$MAE = \frac{1}{n}\sum_{i=1}^{n} |y_i - \widehat{y}_i| \tag{6}$$

$$MSE = \frac{1}{n}\sum_{i=1}^{n} (y_i - \widehat{y}_i)^2 \tag{7}$$

$$MAPE = \frac{1}{n}\sum_{i=1}^{n} \frac{y_i - \widehat{y}_i}{y_i} \times 100 \tag{8}$$

where

y_i is the actual value,

$\widehat{y}_i$ is the predicted value, and

Table 3
Input values before and after scaling.

Pin(bar)		Tin (K)	
Unscaled	Scaled	Unscaled	Scaled
200	0.2785	283.00	0.0900
100	0.1342	300.00	0.2615
300	0.4228	293.15	0.1922
300	0.4228	288.00	0.1401
300	0.4228	293.15	0.1922

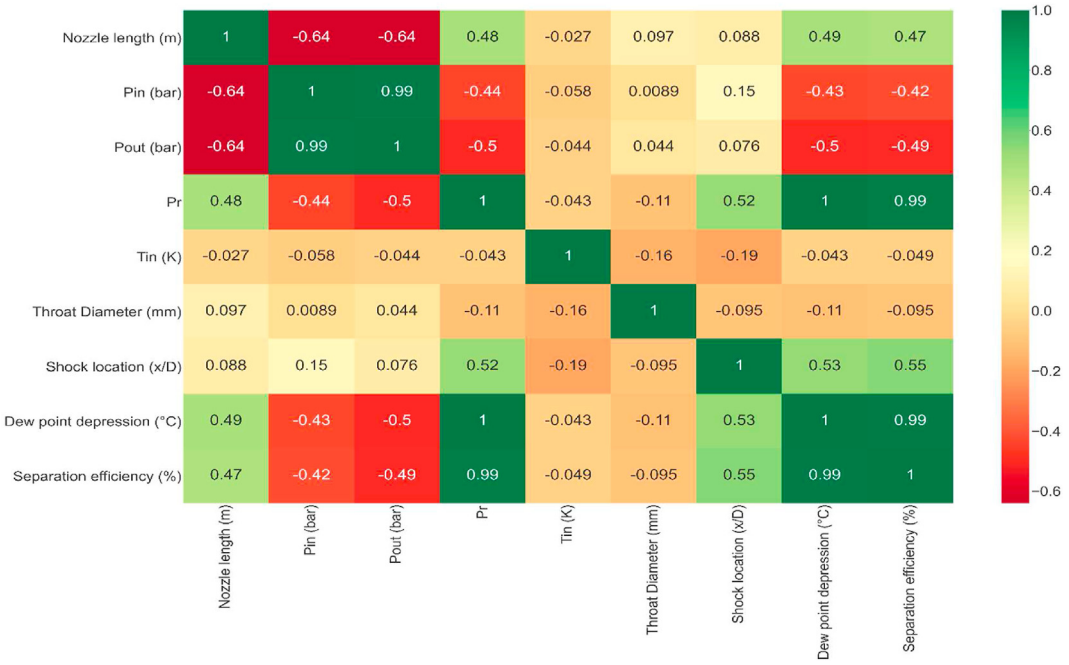

Fig. 5. Correlation matrix for the study.

n is the number of samples.

4. Results and discussion

The nozzle is an important component of a supersonic separator that helps to generate supersonic current and separate the condensate from natural gas stream, thus, the desired nozzle must be clearly designed. The critical area of the nozzle throat determines the mass of gas flow through this device (Yang et al., 2014). During phase change, condensation mainly occurs at the position of the shockwave; the supersonic nozzle geometry configuration is also highly important. The drain location should be aligned with the shockwave location. For each of the target outputs, the decision tree's performance and support vector machines are discussed. The effect of the most crucial input variable in predicting the target output is also addressed under each prediction task. However, discussions for the SVM model are limited by two reasons. Firstly, the decision tree model generally outperformed the SVM model; therefore, the decision tree model is adopted as the model of choice in this study, hence a more thorough discussion is centered around it. Secondly, investigating the SVM model is difficult, that is, it can be difficult to understand why the prediction was made, and the model is often difficult to explain.

4.1. Shockwave location

Shockwaves are formed in the diffuser section of the nozzle. They are responsible for recovering up to 80% of pressure losses. They also aid the separation of phases in the nozzle. Shockwave location is often expressed as a dimensionless parameter i.e. x/D,where

x is the distance between the inlet and the arbitrary cross-section,
D *is* the convergent diameter of x.

4.1.1. Decision tree

References in the literature show that the placement of shock waves has a significant impact on the overall performance of the nozzle and depends to a large extent on the extreme pressure conditions (Shooshtari and Shahsavand, 2013; Vaziri and Shahsavand, 2015). The decision tree model features/important attributes help to identify the variables that are most informative in predicting the target output. The feature importance chart is plotted, and Fig. 6 shows the importance of each variable. The decision tree produced a model with an R^2 value of 0.91 relative to the SVM, for the prediction of shockwave location. This then reveals that the DT model outperforms the SVM model for this prediction task.

The model identified the variables P_r (Pressure loss ratio) and nozzle length as the two most important features for determining the shockwave location inside the supersonic region of the nozzle. Other parameters are either not significant, or that the information they reveal is already considered and accounted for by another variable. The model's feature (variable) importance lies between 0 and 1, with 1 meaning completely informative and 0 being not informative at all. The pressure loss ratio has an importance score of

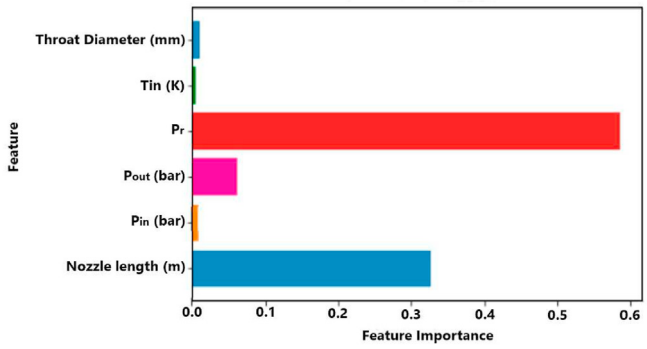

Fig. 6. Feature importance chart for the prediction of shockwave location.

about 0.59, while nozzle length and pressure out have an importance score of about 0.33 and 0.07, respectively. All other input parameters have negligible values.

Ligrani et al. (2020) explained that the shock wave motion generated at the nozzle are caused by large pressure fluctuations when the flow was very turbulent. Pressure fluctuations were also observed at the bottom of the shock wave. The results show that the shockwave's axial position is shifted away from the diffuser as the pressure loss ratio decreases. Also, increasing the pressure loss ratio contributes to a reduction in temperature and pressure. These phenomena (throttling process) have their own advantages and weaknesses in the separation process; the drop in temperature inside the nozzle promotes improved condensation and higher dehydration efficiency. A drop in pressure leads to condensation of the liquid from the gas stream as the temperature drops. On the other hand, large pressure drops cause large pressure losses which poses a serious problem to the pipeing system, especially if the supersonic nozzle is installed inline.

The degree of pressure loss ratio, shock wave, and flow rate has a significant effect on dehydration efficiency (Ding et al., 2020). The normal shock phenomenon usually occurs after the collection point to increase the temperature and pressure the natural gas. According to Niknam et al. (2016), the sensitivity to the shockwave location to pressure boundary values is greater than the temperature boundary values. Due to the non-isentropic behavior of the shock wave, there is a very large pressure difference between the inlet and outlet gas streams. Therefore, it is necessary to select a suitable pressure loss ratio to ensure condensation. This further implies that the degree of randomness of the shockwave/changes in entropy results in large pressure descrepances from the inlet though to the exit of the nozzle. Fig. 7 shows the relationship between the axial shockwave location and the pressure loss ratio. The pressure loss is increased due to the turbulence at the inlet and the large vorticities near the shock wave; this relationship is as illustrated in Fig. 7. The main cause of supersonic nozzle separation is the shock wave, and the trend shows that the shock wave location has a direct relationship with the pressure loss ratio.

The nozzle flow is swift and initially adiabatic with very little friction loss because the flow is one-dimensional, with a favorable pressure gradient, the only exception being when shock waves are generated and nozzles are relatively short. An isentropic pattern in the entire nozzle is, therefore, sufficient for the preliminary design (Papamoschou and Zill, 2004; Naveen et al., 2019). Thus, the variables of state on the onset of condensation depend strongly on the cooling rate of the nozzle. The smaller the radius of curvature and height of the nozzle, the larger the nozzle's cooling rate; thus, the greater the increasing rate of liquid mass fractions (Bolaños-Acosta et al., 2019). With internal supersonic flow, the interaction between the shock wave and the boundary layer is very complex, causing the separation of the boundary layer. When the shockwave is strong enough to separate the boundary layer, the shock wave is bifurcated, and more shockwaves form downstream of the conductive shock wave. The occurrence of asymmetric shockwave systems depend on the area ratio (nozzle outlet and nozzle throat cross-sectional areas). The shockwave asymmetry decreases as the straight nozzle length increases (Matsuo et al., 2012). Table 4 shows a summary of shock wave location prediction using various machine learning algorithms.

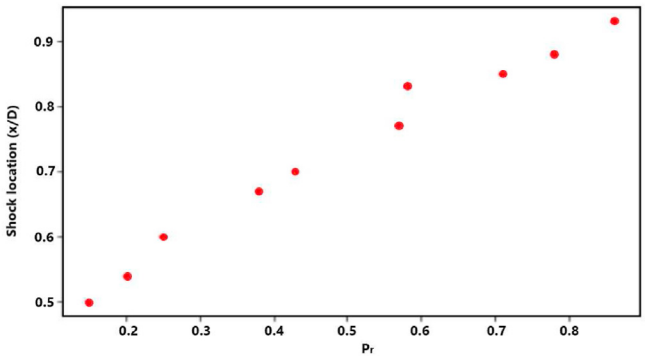

Fig. 7. Shock location vs. pressure loss ratio.

The results from Table 4 shows the prediction error margines for different machine learning algorithms compared with 1-D iterative model from literature. We compare the learning capabilities of these algorithms and optimize the model to reduce the error. Niknam et al. (2016) developed a 1-D inviscid theory model for comparison with predicted experimental data, and this 1-D model was also adoptedin this study for prediction of data. Among the four algorithms used for scaled and unscaled data (Table 4), the 1-D model prediction shows some differences between trends obtained and the results of experimental-based models. This different can be attributed to the simple assumptions made in developing the 1-D model, such as neglecting of swirling effect inside the nozzle. This is because the axial is the only type of flow direction available in this model, while the main velocity elements in the actual process of supersonic nozzles are tangential and axial. As a result, applying high pressure to the same shape improves the equivalent role of axial velocity, which helps to quickly reach the Mach limit required for shockwaves. the accuracy and validity was investigated using two statistical metrics, which are mean square error (MSE) and mean absolute error (MAE).

The length of the nozzle plays an important role in the placement of the shockwaves. A shorter nozzle length can lead to the shockwaves getting too close upstream the nozzle throat, where they can be normalized, thus giving rise to normal waves. On the other hand, the longer the nozzle-length, the farther the shockwave location downstream the nozzle throat (Fig. 8). A longer nozzle length allows for efficient separation of the phases since the shockwave has more space to move within the diffuser without coming too close to the nozzle throat. The larger the nozzle length, the greater the pressure loss ratio and the greater the position of the shockwave from the nozzle throat. Therefore, the larger the position of the shockwave away from the nozzle throat, the higher the pressure loss ratio.

Nozzle length affects the supersonic separation process, and it was observed that a more extended nozzle diffusion section would allow for more axial movement of the shockwave upstream towards the nozzle throat without moving too close to the position where the shockwave would become normalized or oblique, thus causing a re-evaporation of the liquid, leading to poor separation performance of the separator. Since the shockwave location is where the two-phase supersonic flow where $M > 1$ but <5) is converted to single-phase subsonic flow (i.e. $M < 1$) having transitted through the sonic regime (where $M = 1$). However, a better dehydration is achieved when the shockwave occurs closer to the nozzle exit (diffuser section) than at the throat/converging section. This creates more room for condensation.

4.1.2. Support vector machines (SVM)

For the unscaled data, the SVM model gave a R^2 value of 0.13, while a R^2 value of 0.42 was obtained for the scaled data. In lieu of the improvement in the performance of the model when the scaled data was used, the performance was somewhat abysmal, which suggests that the SVM model may not be suitable for the available dataset. This does not leave room for generalization as it may not be the case in all situations but unique to this prediction i.e. the SVM model may perform much better with the other prediction tasks.

Table 4
Machine learning algorithms for predicting shock wave location.

Model	Hyperparameters	Data Scaled?	MSE	MAE
Iterative 1-D model	–	–	1.01e-2	9.86e-2
Support Vector Regressor	C = 1, gamma = 'auto', epsilon = 0.01, coef0 = 0.1, tol = 0.01, max_iter = -1, kernel = 'rbf'	No	Train: 9.0e-5 Test: 2.1e-2	Train: 9.2e-3 Test: 1.3e-1
Support Vector Regressor	C = 10000, gamma = 'auto', epsilon = 0.01, coef0 = 0.001, tol = 0.00001, max_iter = -1, kernel = 'rbf'	Yes	Train: 9.4e-5 Test: 4.9e-3	Train: 9.5e-3 Test: 5.7e-2
Random Forest Regressor	max_depth = None, criterion = "mae", n_estimators = 1000, max_features = 'auto', n_jobs = -1, ccp_alpha = 0.001	No	Train: 1.0e-3 Test: 2.2e-3	Train: 2.6e-2 Test: 4.1e-2
Random Forest Regressor	max_depth = None, random_state = 0, criterion = "mae", n_estimators = 1000, max_features = 'auto', n_jobs = -1, ccp_alpha = 0.001	Yes	Train: 1.05e-3 Test: 1.99e-3	Train: 2.6e-2 Test: 3.8e-2
Gradient Boosting Regressor	n_estimators = 1000, learning_rate = 0.1, max_depth = None, loss = 'ls'	No	Train: 1.0e-7 Test: 1.6e-3	Train: 2.5e-4 Test: 3.6e-2
Gradient Boosting Regressor	n_estimators = 1000, learning_rate = 0.1, max_depth = None, random_state = 0, loss = 'ls'	Yes	Train: 1.0e-7 Test: 1.3e-3	Train: 2.5e-4 Test: 3.2e-2
Extra Trees Regressor	n_estimators = 1000, ccp_alpha = 0.0	No	Train: 0.0 Test: 1.0e-3	Train: 0.0 Test: 2.7e-2
Extra Trees Regressor	n_estimators = 1000, ccp_alpha = 0.0	Yes	Train: 0.0 Test: 1.0e-3	Train: 0.0 Test: 2.7e-2

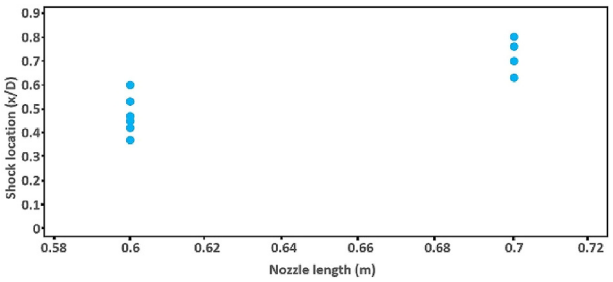

Fig. 8. Effect of Nozzle Length on Shock location.

4.2. Dew point depression

4.2.1. Decision tree

The decision tree produced a model with R^2 value of 0.97 for the prediction of dewpoint depression. It slightly gave a lower degree of model-data matching relative to the SVM model, and Fig. 9 shows the feature importance plot. It is the only case where the SVM model outperforms the decision tree model. Increasing the gas pressure also increases the dew point temperature.

The model identifies the P_r (Pressure loss ratio) variable as the most informative feature in predicting dew point depression. If the pressure increases, the mass of liquid vapour per volume unit of gas must be reduced to maintain the same dew point. This is important because changes in gas pressure lead to changes in its saturation points. The pressure loss ratio has a feature importance score of 0.69, while the outlet and inlet pressure have scores of 0.22 and 0.08, respectively. All other parameters either have a score of zero or are negligible. Fig. 9 shows that the effect of inlet and outlet pressures on the dew point depression is much smaller than the extent of the pressure loss ratio, especially at constant pressure loss ratio; which shows that the effect of the inlet pressure on the gas dew point separation is small at a fixed pressure loss ratio. Cao and Yang (2015) studied the effect of inlet and outlet pressures and found that as the pressure loss ratio increased, the dew point depression decreases with inlet pressure. In addition, the effect of the outlet pressure on the dew point depression is minimal. Fig. 10 shows a graph of dew point depression against pressure loss ratio. It can be seen that when the pressure loss ratio increases to 0.7, the dew point depression increases to about 52.04 °C. This means that for supersonic separation, the highest dew point depression is achieved when operating at greater pressure loss ratio.

For a fixed outlet pressure, an increase in the inlet pressure increases the pressure loss ratio, leading to an increase in dew point depression. However, based on literature, high inlet pressures of the flowing gas creates a supercritical fluid in the supersonic separator, which causes serious problems in gas dehydration (Yang et al., 2014). Also, a decrease in the outlet pressure increases the pressure loss ratio for fixed inlet pressure. The lower the outlet pressure compared to the inlet pressure, the higher the pressure loss ratio, and the greater the dew point depression. Hence a remarkably low outlet pressure will result in a higher dew point depression, suitable for gas dehydration (Fig. 11).

4.2.2. Support vector machines (SVM)

Using the unscaled data, the SVM model gave a R^2 value of 0.97 while it gave a value of 0.99 for the scaled data. This shows a moderate improvement in the model's performance, and it also outperforms the decision tree model for the predicted relationships of these test parameters. Of all the cases examined, this remains the only case where the performance of the SVM model exceeds that of the decision tree model.

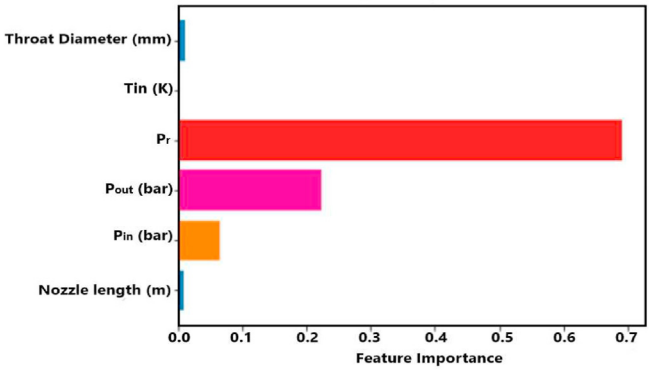

Fig. 9. Nozzle conditions and their predictive influence on the process.

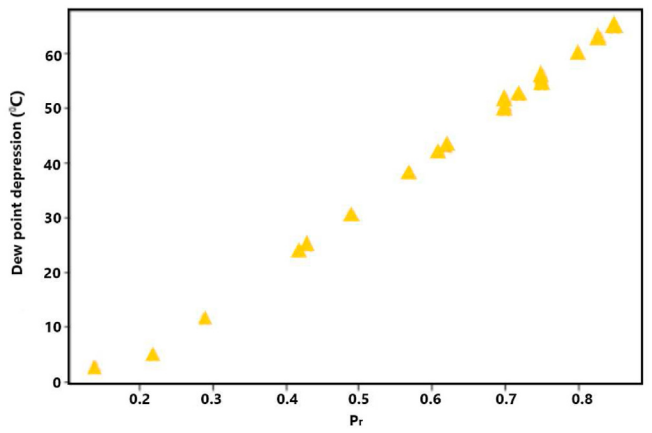

Fig. 10. Dew point depression vs. Pressure loss ratio.

4.3. Separation efficiency

4.3.1. Decision tree

From Fig. 12 analysis, the decision tree produced a model with R^2 value of 0.97 for the prediction of separation efficiency, hence it outperformed the SVM model. The model identifies the Pr (Pressure loss ratio) variable as the most informative feature in predicting the separation performance of the supersonic separator. The pressure loss ratio has a feature importance score of 0.84, while throat diameter has a score of 0.14. As the pressure loss ratio increases with the swirling length, the supersonic separator provides better dehydration performance. The higher the inlet pressure loss ratio, the higher the separation efficiency and vice versa. Xingwei et al. (2015) also concluded that pressure loss and the swirling length ratios have proved to play significant roles in improving the swirling separation effect. However, changing the inlet pressureat the nozzle changes the hydrodynamics of the gas stream, which

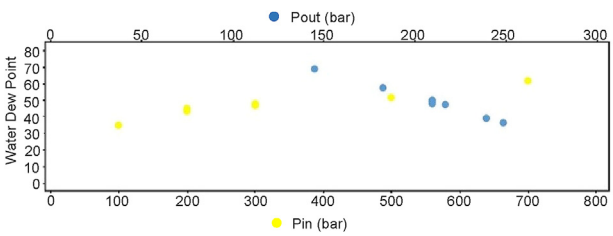

Fig. 11. Comparing the effect of Inlet and outlet pressure on dew point depression.

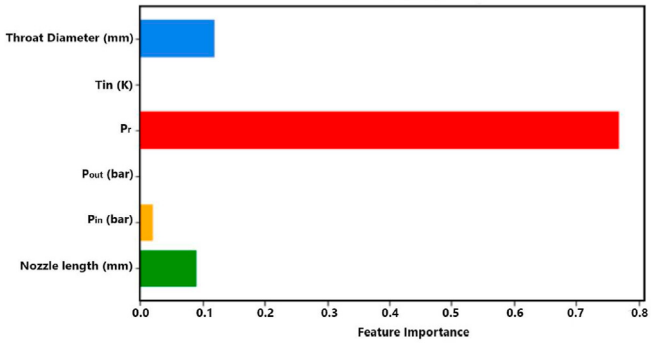

Fig. 12. Feature importance chart for the prediction of separation efficiency.

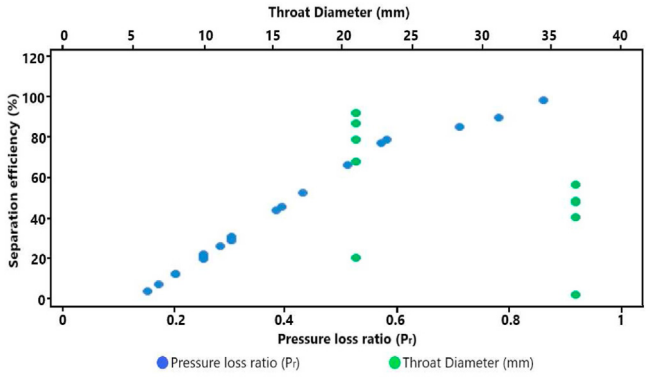

Fig. 13. Pressure loss ratio and throat diameter on separation efficiency.

reduces the separation efficiency.

The flow at the nozzle throat occurs at sonic velocity while condensation and separation occur at a supersonic rate in the diverging section of the nozzle, which is located after the nozzle throat. Fig. 13 shows that a higher pressure loss ratio will give a better separation efficiency, as a pressure loss ratio of 0.6 will give a separation efficiency of about 80%. However, at still higher pressure loss ratios, pressure losses become more pronounced, which may be undesirable for field operations. A lower pressure loss ratio, on the other hand, can still give suitable dehydration performance while minimizing pressure losses. As stated earlier, a pressure loss ratio of 0.6 ensures a balance between ensuring good separation and minimizing pressure losses.

The condensation of liquids in the gas is made possible due to the expansion of the gas as it moves downstream from the nozzle

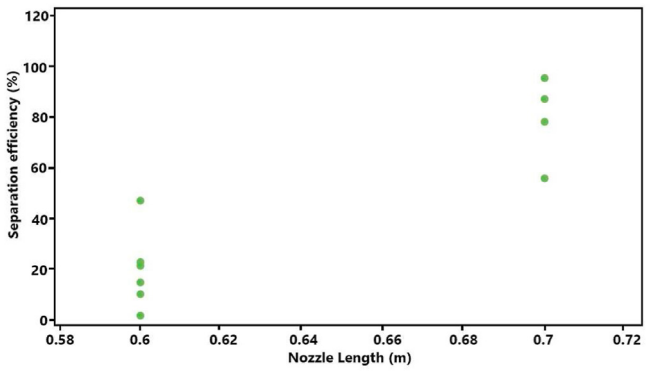

Fig. 14. Separation efficiency vs. Nozzle.

Table 5
Summary of the performance of each model.

R^2 Score			
	Decision tree	SVM (unscaled)	SVM (scaled)
Shock wave location	0.91	0.13	0.42
Dew point depression	0.97	0.97	0.99
Dehydration efficiency	0.97	0.87	0.93

Table 6
Effects and relationship of the parameters to separation process.

Parameters	Shock wave location	Dew point suppression	Dehydration efficiency
P_r	Highly significant and directly related	Highly significant and directly related	Very significant and directly related
Nozzle Length	Significant and directly related	Insignificant	Very significant and related
Throat diameter	Insignificant	Insignificant	Significant and inversely related

throat. The sudden increase in the nozzle diameter after exiting the nozzle throat is responsible for the condensation due to expansion. A relatively smaller throat diameter than the diameter downstream the nozzle throat will result in a greater condensation of liquids due to rapid gas expansion (Fig. 13) which in turn gives higher separation efficiencies. Fig. 14 shows that a nozzle length of 0.7 gives a better separation performance than a nozzle length of 0.6. Wen et al. (2011) used the discrete particle method and found that a longer nozzle length gives better separation efficiency. A nozzle length ten times the throat diameter's size was recommended in that study.

4.3.2. Support vector machines (SVM)

For the unscaled data, using the SVM model, a R^2 value of 0.87 was obtained, while it gave a R^2 value of 0.93, when used to treat the scaled data (Table 5). Hence, there is a moderate improvement in the efficiency of the model when the scaled dataset is used. Despite this improvement, the model did not outperform the decision tree model for the tested data. For the dew point depression prediction using the scaled data, the SVM model performed better than the decision tree model. The decision tree model outperformed the SVM model for the other two target outputs (shockwave location and separation efficiency), while taking into cognizance, the inferior performance of the SVM model in predicting shockwave location (that is, R^2 scores of 0.13 and 0.42 for the unscaled and scaled data, respectively). Given that the decision tree model consistently showed good performance across all three output predictions, it was adopted as the chosen model for this study.

5. Summary of the findings

It is essential to understand the relationship between input variables and target outputs. This understanding of how each input variable affects the target output helps to determine how to design an efficient nozzle and maintain optimal gas separation in the event of unstable input parameters. The relationship between the selected input variables and target outputs are shown in Table 6. In this case, the effects of P_{out} and P_{in} on the target outputs are assumed to be captured by the pressure loss ratio P_r.

The widespread use of numerical models suggests a broad acceptance of their performance and reliability; thus, they can be taken as a benchmark to assess the performance of any other model. Table 7 shows the results of the evaluation obtained as a statistical result. This clearly shows that the Decision tree model is superior in this case study to the 1-D isentropic flow model developed by LeMartelot et al. (2013). The one-dimensional analysis assumes that the shock is normal and that the flow through the shock sticks to the wall. When the Mach number is less than 1 (that is, $M < 1$), the subsonic flow after the shockwave extends isentropically to the back pressure level at the nozzle outlet. However, the flow separates from the wall and forms a separation zone; subsequently, the flow becomes unstable and heterogeneous (Padmanathan and Vaidyanathan, 2012).

Based on the results presented in Table 7, the 1-D model (Niknam et al., 2016) gives more unsatisfactory performances, probably due to a simple assumption of neglecting the nozzle's swirling effect. Important phenomena such as phase changes and gas condensation are also ignored in the numerical modeling procedure, hence, the model's failure to handle two-phase conditions. These are serious disadvantages, as multiphase compressible swirling currents can cause phase changes under high-pressure conditions and most numerical models do not cover all these aspects. Another disadvantage of numerical approaches is that it requires precise system details, which may not appear in many real applications. The machine learning models, such as the decision tree used in this study are designed to overcome some of these limiting requirements.

Unlike previous numerical models, the proposed model covers a number of threshold conditions that reveal the stimulating effect of pressure loss ratio. In addition, the previously neglected role of the swirling effect is reported in the appropriate experimental dataset. Furthermore, using the decision tree as a black-box model significantly reduces its computational complexity.

Table 7
Statistical error analysis.

	MAPE	MSE	RMSE	MAE
Decision tree model	5.98	2.30E-03	4.80E-02	4.31E-02
Iterative 1-D model	15.44	1.01E-02	1.00E-01	9.86E-02

6. Conclusions

The most significant parameters affecting the supersonic separation device have been investigated and presented. This was achieved using the decision tree machine learning model on supersonic separation data published in literature. The machine learning model-accuracy and reliability were validated by comparing it with an existing 1-D iterative model alongside the SVM. The conclusions are as follows:

(1) The machine learning model was more accurate than the 1-D Iterative model with a MAPE of 5.98 compared to 15.44.
(2) Shock wave location is mainly affected by pressure loss ratio and nozzle length.
(3) The pressure loss ratio is the most significant parameter affecting the dew point depression.
(4) The separation efficiency is mainly dependent on the pressure loss ratio, nozzle throat diameter, and the nozzle length.
(5) The best pressure loss ratio of 0.6 was found to give a suitable dehydration performance of 80% while minimizing pressure losses.

CRediT authorship contribution statement

Emmanuel E. Okoro: Software, Supervision. **Uyiosa Igbinedion:** Conceptualization, Methodology, Software, Validation, Investigation. **Victor Aimikhe:** Methodology, Writing – original draft. **Samuel E. Sanni:** Methodology, Formal analysis, Investigation, Writing – review & editing. **Okorie E. Agwu:** Conceptualization, Validation, Formal analysis, Investigation, Writing – original draft, Writing – review & editing.

Declaration of competing interest

The authors declare that they have no known competing financial interests or personal relationships that could have appeared to influence the work reported in this paper.

References

Alnoush, W., Castier, M., 2019. Shortcut modeling of natural gas supersonic separation. J. Nat. Gas Sci. Eng. 65, 284–300. https://doi.org/10.1016/j.jngse.2019.03.004.

Bian, J., Cao, X., Yang, W., Song, X., Xiang, C., 2019. Condensation characteristics of natural gas in the supersonic liquefaction process. Energy. 168, 99–110.

Bolaños-Acosta, A.F., T-Rodrigues, C., Restrepo-Lozano, J.C., Simoes-Moreira, J.R., 2019. Condensation and Normal Shock Wave Location in Supersonic Nozzles. In: 25th ABCM International Congress of Mechanical Engineering. Uberiandia, MG, Brazil.

Cao, X., Yang, W., 2015. The dehydration performance evaluation of a new supersonic swirling separator. J. Nat. Gas Sci. Eng. 27, 1667–1676.

Cao, X., Bian, C., 2019. Supersonic separation technology for natural gas processing: a review. Chem. Eng. Process. 138, 138–151.

Castier, M., 2014. Modeling and simulation of supersonic gas separations. J. Nat. Gas Sci. Eng. 18, 304–311.

Ding, H., Sun, C., Wang, C., Wen, C., Tian, Y., 2020. Prediction of dehydration performance of supersonic separator based on amulti-fluid model with heterogeneous condensation. Appl. Therm. Eng. 171, 115074.

Jing, H.A.N., Ran, D.U.A.N., Meng, W.U., 2014. Performance of dual-throat supersonic separation device with porous wall structure. Chin. J. Chem. Eng. 22 (4), 370–382.

Karimi, A., Abdi, M.A., 2009. Selective dehydration of high-pressure natural gas using supersonic nozzles. Chem. Eng. Process. Process Intensify. 48 (1), 560–568.

LeMartelot, S., Saurel, R., LeMetayer, O., 2013. Steady one-dimensional nozzle flow solutions of liquid-gas mixtures. J. Fluid Mech. 737, 146–175.

Ligrani, P.M., McNabb, E., Collopy, H., Anderson, M., Marko, S.M., 2020. Recent investigations of shock wave effects and interactions. Adv. Aerodynam. 2, 4. https://doi.org/10.1186/s42774-020-0028-1.

Mahmoodzadeh Vaziri, B., Shahsavand, A., 2013. Analysis of supersonic separators geometry using generalized radial basis function (GRBF) artificial neural networks. J. Nat. Gas Sci. Eng. 13, 30–41.

Marcelo, M., 2016. Neural network for percipitation analysis in a humid region to detect drought and wet year alams. Met. Apps. 24, 8–18.

Matsuo, S., Kanesaki, K., Nagao, J., Khan, M.T.I., Setoguchi, T., Kim, H.D., 2012. Effects of supersonic nozzle geometry on characteristics of shock wave structure. Open J. Fluid Dynam. 2, 181–186.

Naveen, K.K., Vijayanandh, R., Ramesh, M., 2019. Design optimization of nozzle and second throat diffuser system for high altitude test using CFD. J. Phys. Conf. 1355.

Netusil, M., Ditl, P., 2012. Natural Gas Dehydration, Natural Gas - Extraction to End Use. Sreenath Borra Gupta, IntechOpen. https://doi.org/10.5772/45802.

Niknam, P.H., Mokhtarani, B., Mortaheb, H.R., 2016. Prediction of shockwave location in supersonic nozzle separation using self-organizing map classification and artificial neural network modeling. J. Nat. Gas Sci. Eng. 34, 917–924.

Niknam, P.H., Mortaheb, H.R., Mokhtarani, B., 2018a. Effects of fluid type and pressure order on performance of convergent-divergent nozzles: an efficiency model for supersonic separation. Asia Pac. J. Chem. Eng. 13 (2), e2181. https://doi.org/10.1002/apj.2181.

Niknam, P.H., Mortaheb, H.R., Mokhtarani, B., 2018b. Dehydration of low-pressure gas using supersonic separation: experimental investigation and CFD analysis. J. Nat. Gas Sci. Eng. 52, 202–214.

Niknam, P.H., Fiaschi, D., Mortaheb, H.R., Mokhtarani, B., 2019. Numerical investigation of multiphase flow in supersonic separator considering inner body effect. Asia Pac. J. Chem. Eng. e2380. https://doi.org/10.1002/apj.2380.

Okimoto, F., Brouwer, J.M., 2002. Supersonic gas conditioning. World Oil. 223, 89–92.

Othman, N.A., Tufa, L.D.M., Zabiri, H., Md Jalil, A.-M., Rostani, K., 2020. Enhancing the Supersonic Gas Separation operating envelope through process control strategies of the feed conditioning plant for offshore CO_2 removal from natural gas. Int. J. Greenhouse Gas Control. 94, 102928. https://doi.org/10.1016/j.ijggc.2019.102928.

Padmanathan, P., Vaidyanathan, S., 2012. Computational analysis of shockwave in convergent divergent nozzle. Int. J. Eng. Res. Afr. 2 (2), 1597–1605.

Papamoschou, D., Zill, A., 2004. Fundamental Investigation of Supersonic Nozzle Flow Separation. American Institute of Aeronautics and Astronautics, Inc., Reston.

Ruiz, S., 2015. Natural gas and CO2 separation units. Science. 213, 952–965.

Sanni, S.E., Agboola, O., Fagbiele, O., Yusuf, E.O., Emetere, M.E., 2020. Optimization of natural gas treatment for the removal of CO_2 and H_2S in a novel alkaline-DEA hybrid scrubber. Egypt. J. Petrol. 29 (1), 83–94.

Shooshtari, S.R., Shahsavand, A., 2013. Reliable prediction of condensation rates for purification of natural gas via supersonic separators. Separ. Purif. Technol. 116, 458–470.

Vaziri, B.M., Shahsavand, A., 2015. Optimal selection of supersonic separators inlet velocity components via maximization of swirl strength and centrifugal acceleration. Separ. Purif. Technol. 50 (5), 752–759.

Wajdi, A., Marcelo, C., 2019. Shortcut modeling of natural gas supersonic separation. J. Nat. Gas Sci. Eng. 65, 284–300.

Wang, Y., 2020. Analysis for spiral vortex and effect of profile of nozzle and swirler on performance of supersonic separator. Chem. Eng. Process. 147, 107676.

Wen, C., Cao, X., Yang, Y., Zhang, K., 2011. Swirling effects on the performance of supersonic separators for natural gas separation. Chem. Eng. Technol. 34, 1575–1580.

Xiao, Q., Tsai, H.M., Papamoschou, D., Johnson, A., 2009. Experimental and numerical study of jet mixing from a shock-containing nozzle. J. Propul. Power. 25 (3), 688–696.

Xingwei, L., Zhongliang, L., Yanxia, L., 2015. Numerical study of the high speed compressible flow with non-equilibrium condensation in a supersonic separator. J. Clean Energy Technol. 3 (5), 360–366.

Xuewen, C., Jiang, B., 2019. Supersonic separation technology for natural gas processing: a review. Chem. Eng. Process. 136, 138–151.

Yang, Y., Wen, C., Wang, S., Feng, Y., 2014a. Effect of inlet and outlet flow conditions on natural gas parameters in supersonic separation process. PLoS One. 9 (10), e110313. https://doi.org/10.1371/journal.pone.0110313.

Yang, Y., Wen, C., 2017. CFD modeling of particle behavior in supersonic flows with strong swirls for gas separation. Separ. Purif. Technol. 174, 22–28.

Yang, Y., Wen, C., Wang, S., Feng, Y., 2014b. Numerical simulation of real gas flows in natural gas supersonic separation processing. J. Nat. Gas Sci. Eng. 21, 829–836.

Yang, Y., Wen, C., Wang, S., Feng, Y., 2014. Effect of inlet and outlet flow conditions on natural gas parameters in supersonic separation process. PLoS ONE. 9 (10), e110313.

Zhang, S., Zhou, Z.N., Li, Y.M., Wang, L., Liu, C., 2014. Mathematically based study of condensing flow based model. Appl. Them. Eng. 98, 929–938.